

Document downloaded from:

<http://hdl.handle.net/10251/85372>

This paper must be cited as:

Bronchalo, E.; Coves, A.; Mata Sanz, R.; Gimeno Martinez, B.; Montero, I.; Galán, L.; Boria Esbert, VE.... (2016). Electron Emission of Pt: Experimental Study and Comparison With Models in the Multipactor Energy Range. IEEE Transactions on Electron Devices. 63(8):3270-3277. doi:10.1109/TED.2016.2580199.



The final publication is available at

<http://doi.org/10.1109/TED.2016.2580199>

Copyright Institute of Electrical and Electronics Engineers (IEEE)

Additional Information

"(c) 2016 IEEE. Personal use of this material is permitted. Permission from IEEE must be obtained for all other users, including reprinting/ republishing this material for advertising or promotional purposes, creating new collective works for resale or redistribution to servers or lists, or reuse of any copyrighted components of this work in other works."

Secondary Electron Emission of Pt: Experimental Study and Comparison with Models in the Multipactor Energy Range

Enrique Bronchalo, Ángela Coves, Rafael Mata, Benito Gimeno *Member, IEEE*, Isabel Montero, Luis Galán, Vicente E. Boria *Senior Member, IEEE*, Laura Mercadé and Esteban Sanchís *Senior Member, IEEE*

Abstract—Experimental data of secondary emission yield (SEY) and electron emission spectra of Pt under electron irradiation for normal incidence and primary energies lower than 1 keV are presented. Several relevant magnitudes, as total SEY, elastic backscattering probability, secondary emission spectrum (SES) and backscattering coefficient, are given for different primary energies. These magnitudes are compared with theoretical or semiempirical formulas commonly used in the related literature.

Index Terms—multipactor, Secondary Emission Yield, backscattered electrons, secondary emission spectrum.

I. INTRODUCTION

THE theoretical and experimental research on secondary emission is important not only from a fundamental point of view, but also for many practical applications. Among others, we can mention multipactor effects in space-borne RF devices [1], [2], multipactor in RF-vacuum windows [3], [4], multiplication processes in photomultipliers and multichannel plates [5], electron microscopy techniques [6], [7], charging effects on spacecraft surfaces [8], [9] and dust grain charging in space plasmas [10]. A detailed description of electron emission under electron bombardment should cover the energy and angular dependence of the different contributions to the electron emission yield (secondaries, elastically and inelastically backscattered electrons) and their spectral and angular distributions. Many theoretical and experimental works have addressed those issues in the last 60 years [6], [11]–[15]. However, there is still a lack of a global and unified description of the different aspects of the secondary emission problem.

In this context, the aim of this work is to check the validity of several approaches to the secondary emission yield (SEY) and secondary emission spectrum (SES) dependence with the electron primary energy. Our main interest is to find reliable

expressions that can be used in multipactor simulation problems. We have limited our study to electron normal incidence and to energies lower than 1 keV, which is the typical energy range in multipactor discharges. We have chosen Pt as test material to best compare the results with other publications because of its low reactivity, since surface contamination can alter strongly the secondary emission properties.

The paper is organized as follows: the relevant magnitudes used along the paper are defined in Section II. In Section III we expose the experimental setup and the details of the measurement process. Section IV is devoted to the SEY results and the comparison with several models. In Section V, the SES characteristics, the elastic contribution to the yield and the backscattering coefficient are exposed and compared with several parameterizations. The main conclusions obtained in this work are summarized in Section VI.

II. DEFINITION OF THE RELEVANT MAGNITUDES

Before describing the SEY measurement process, we define the relevant magnitudes used along the paper. The total SEY, including all electrons emitted by the sample, is defined as the ratio of the emission current to the primary electron current impinging on the sample:

$$\sigma = \frac{I(\text{emitted } e^-)}{I(\text{primary } e^-)}. \quad (1)$$

The total SEY includes two contributions: true secondary electrons (δ) and backscattered electrons (η):

$$\sigma = \delta + \eta. \quad (2)$$

As there is no unambiguous distinction between the low-energy backscattering emission and the true secondary emission, an energy of 50 eV is commonly admitted by convention as the frontier between the secondary spectrum and the lower side of the backscattering spectrum for primary energies E_p higher than ≈ 100 eV. Therefore, the contribution of the backscattered electrons to the yield is

$$\eta = \frac{I(\text{emitted } e^-, E > 50 \text{ eV})}{I(\text{primary } e^-)}. \quad (3)$$

The backscattering yield is commonly known as backscattering coefficient. An additional distinction, convenient for the purposes of this paper, can be made between the elastic and inelastic contribution to the backscattering yield:

$$\eta = \eta_e + \eta_i. \quad (4)$$

E. Bronchalo and Á. Coves are with the Department of Communications Engineering, Universidad Miguel Hernández de Elche, Elche, 03202 Spain e-mail: ebronchalo@umh.es.

R. Mata, B. Gimeno and L. Mercadé are with the Department of Applied Physics and Electromagnetism-ICMUV, Universidad de Valencia, Burjassot, 46100 Spain.

I. Montero is with the Institute of Material Sciences of Madrid, Madrid, 28049 Spain.

L. Galán is with the Department of Applied Physics, Universidad Autónoma de Madrid, Madrid, 28049 Spain.

V.E. Boria is with the Department of Communications-iTEAM, Universitat Politècnica de València, Valencia, 46022 Spain.

E. Sanchís is with the Department of Electronics Engineering, Universidad de Valencia, Burjassot, 46100 Spain.

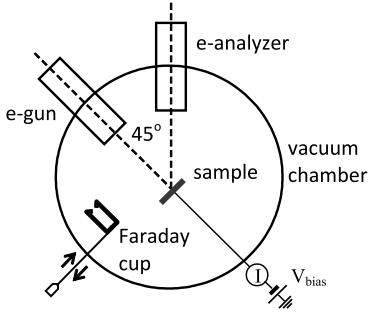


Fig. 1. Experimental setup.

Electrons with energies corresponding to the elastic peak are accounted for in η_e , whereas electrons with energies between 50 eV and the elastic peak, referred to as inelastically backscattered or rediffused electrons, are accounted for in η_i .

It is also convenient to introduce the elastic fraction, f_e , which is the ratio of elastic events in the elastic peak to the total number of events in the emission spectrum. An analogous definition is valid for the inelastic and the true secondary fractions, f_i and f_s respectively. Obviously, $f_e + f_i + f_s = 1$. The relations between the yields and the fractions are straightforward:

$$\left. \begin{aligned} \eta_e &= f_e \sigma \\ \eta_i &= f_i \sigma \\ \delta &= f_s \sigma \end{aligned} \right\}. \quad (5)$$

III. EXPERIMENTAL SETUP AND MEASUREMENT PROCESS

The measurements were done in the laboratories of European Space Agency - Val Space Consortium (Valencia, Spain), and Institute of Material Sciences - CSIC (Madrid, Spain). The scheme of the measurement setup is shown in Fig. 1. The solid angle covered by the analyzer is $\Delta\Omega \approx 0.16$ sr. The sample is a 10×10 mm² square sheet of polycrystalline Pt with a purity of 99.999 %. It was cleaned with an Ar⁺ ion beam of 3 keV and a current of 0.7 μ A for 25 minutes at $1.3 \cdot 10^{-7}$ mbar vacuum level. To assure the stabilization of the primary current, the e-gun was turned on for 16 hours before any measurement was made, keeping the sample away from the beam.

The measurements were done at normal incidence and at a vacuum level of 10^{-9} mbar. Three types of measurements were carried out: total SEY, backscattered yield and SES. In all measurements, the primary energies were referred to the sample position by adding (positive bias) or subtracting (negative bias) to the beam energy the electrostatic energy $|eV_{bias}|$ due to the sample bias.

For the total SEY measurement, the sample was biased at a negative potential of -28.3 V to ensure that all electrons emitted by the sample or by other surfaces (after collisions of backscattered electrons) do not return to the sample. A battery box was used to ensure a very stable bias. The high conductivity of Pt prevents charge accumulation in the sample, and therefore the sample potential was kept constant during the experiment. The total SEY was calculated using eq. (1), where the current of emitted electrons was obtained as the difference between the primary beam current and the bias

current to ground. The energy of primary electrons was varied from 2 eV to about 970 eV in 5 eV steps. The primary beam current for these energies was measured with a Faraday cup before the sample was placed in the electron beam line.

A similar procedure, using eq. (3), was used to measure the yield due to electrons backscattered out of the sample by elastic or inelastic collisions. In this case, the sample was polarized with a positive bias voltage of +50 V. In this way, true secondary electrons are recaptured by the sample, and therefore they do not contribute to the emission current. Under these conditions, the difference between the primary current and the bias current provides the emission current due only to backscattered electrons.

For the measurements of the SES, the electron spectrometer was set to 45° relative to the sample normal (Fig. 1). In our equipment, the angle between the e-gun and the spectrometer is fixed to 45°, so that the beam incidence angle determines the spectrometer line-of-sight. Several negative bias voltages were tried, keeping the beam energy constant, and the recorded spectra were compared. It was observed that for high sample bias the low-energy (i.e., true secondary) contribution to the spectra were significantly reduced. This is explained by the focusing effect of the bias field, as pointed out by Endo and Ino [16] and by Nickles et al. [9]. The bias field is nearly normal to the sample in the region surrounding it, and thus the emitted electrons deviate from their original emission angle towards the normal. This effect is especially important for very low energies. The relation between emitted and detected distributions is not easy to establish, as it would require a precise knowledge of the field geometry in the region between the sample and the spectrometer. However, an approximate relation can be obtained supposing that the ratio of the electrostatic energy eV_{bias} which goes to increase the electron kinetic energy in the normal direction is independent of the emission energy and angle. This simplification leads to the following relation between emitted and detected energy distributions:

$$\left(\frac{dN}{dE}\right)_{detected} \cong C \sqrt{1 - \frac{E_{min}}{E}} \left(\frac{dN}{dE}\right)_{emitted}. \quad (6)$$

In eq. (6), E_{min} is the minimum electron energy that can be detected at the spectrometer position, corresponding to electrons emitted parallel to the sample surface. The constant C is determined by the spectrometer angle and acceptance solid angle. To derive eq. (6), we have assumed a $\cos\theta$ emission law [15], as commonly accepted for the true secondary component. For a radial field, E_{min} can be shown to be zero, and no focusing effect occurs. In general, E_{min} is proportional to the bias voltage, and therefore low bias is required to avoid distortion of the spectra.

Using eq. (6) as a qualitative tool to study the measured spectra for different sample bias, we have estimated that, for our measurement setup, very low distortion can be achieved keeping $|V_{bias}|$ lower than 20 V. Finally, a negative polarization of 19.3 V was used in the spectra measurements. The emission spectra were recorded for ten primary energies logarithmically spaced between 40 and 820 eV relative to the sample vacuum level.

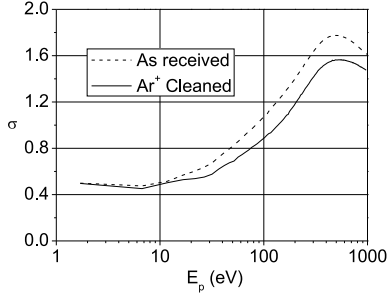


Fig. 2. Total yield measured for Pt as a function of primary electron energy.

TABLE I
EXPERIMENTAL TOTAL SEY (σ) PARAMETERS FOR THE PT SAMPLE

	E_m (eV)	σ_m	E_1 (eV)
As received	500	1.78	84
Ar ⁺ cleaned	530	1.56	137

IV. SECONDARY EMISSION YIELD: EXPERIMENTAL RESULTS AND COMPARISON WITH PARAMETERIZATIONS

The total yield was measured for a Pt foil as a function of primary electron energy as described in Section III. The results are plotted in Fig. 2 for the sample as received and after cleaning by Ar⁺ bombardment. Some relevant parameters of the SEY curve are the maximum yield σ_m , the primary energy of maximum yield, E_m , and the first energy for which the yield is equal to one, E_1 . The second energy for which $\sigma = 1$ is beyond the highest energy in our measurements (970 eV). The experimental values of these parameters, before and after Ar⁺ cleaning, are shown in Table I.

The true secondary yield curve, $\delta(E_p)$, has been obtained from the total SEY data by subtracting the backscattered contribution, measured as described in Section II. The maximum secondary yield, δ_m , and the corresponding energy, E_m , are given in Table II along with the results extracted from the SEY curve of Walker et al. [17] and the Pt data of Lin and Joy database [14]. The value of E_m extracted from the curve of Walker is approximate, as the maximum of the SEY curve is rather flat. Although we have used the symbol E_m in tables I and II for the energies corresponding to the maximum of $\sigma(E_p)$ and $\delta(E_p)$, respectively, on what follows E_m refers always to $\delta(E_p)$. The lower δ_m value obtained for the cleaned sample, as compared with the values of Walker et al. and Lin and Joy, along with the significant reduction in σ_m after cleaning, suggests a surface roughness increase due to the Ar⁺ bombardment, in consistency with reported experimental works (see for instance [18]).

Next, we pass to compare the energy dependence of the measured secondary yield with several parameterizations commonly found in the related literature.

Probably the most frequently used expression for the SEY is the semiempirical universal law:

$$\frac{\delta(E_p)}{\delta_m} = Ax^{1-n}(1 - e^{-bx^n}) \quad (7)$$

TABLE II
TRUE SECONDARY YIELD (δ): COMPARISON BETWEEN EXPERIMENTAL PARAMETERS

	E_m (eV)	δ_m
This work	470	1.27
Walker [17]	740	1.36
Lin and Joy [14]	550	1.69

where $x \equiv E_p/E_m$ is the primary energy normalized to the energy of maximum SEY, and where A and b are constants determined by the parameter n through the conditions $\delta(E_m) = \delta_m$ and $(d\delta/dE)_{E_m} = 0$. This expression is based on three assumptions: a) the energy lost per unit length by the incoming electron is constant along the trajectory; b) the path length-primary energy relation follows a power-law; c) the escape probability for secondary electrons decreases exponentially with the generation depth.

As far as we know, the previous expression was first used by Lye and Dekker [11] with $n = 1.35$, the same value used later by Seiler [6]. Lin and Joy [14] chose $n = 1.67$ and the constants $b = 1.614$ and $A = 1.28$, the last one probably by mistake, as the resultant normalized yield is slightly higher than one. More sophisticated versions of the theory have been developed by Clerc et al. [19] and by Bundaleski et al. [20].

Another commonly used formula for the SEY was proposed by Vaughan [21], [22]:

$$\frac{\delta(E_p)}{\delta_m} = \begin{cases} (x \cdot e^{1-x})^k, & x \leq 3.6 \\ \frac{1.125}{x^{0.85}}, & x \geq 3.6. \end{cases} \quad (8)$$

In this case, the normalized energy is defined in a slightly different way:

$$x = \frac{E_p - E_0}{E_m - E_0}$$

where E_0 is taken as 12.5 eV. The other parameter of the model is:

$$k = \begin{cases} 0.56 & x \leq 1 \\ 0.25, & x > 1. \end{cases}$$

It can be seen that the asymptotic behavior of Vaughan parameterization and semiempirical universal law are the same. In the low-energy region, the Vaughan parameterization is not defined below E_0 .

Furman and Pivi [23], in an extension of previous works, propose

$$\frac{\delta(E_p)}{\delta_m} = \frac{nx}{n - 1 + x^n} \quad (9)$$

with $x = E_p/E_m$ and $n = 1.35$. For very high or very low energies, this functional dependence is the same as the universal law, except for a factor.

The fourth and last parameterization that we will consider here is the one proposed by Scholtz et al. [13]:

$$\frac{\delta(E_p)}{\delta_m} = e^{-\frac{\ln^2 x}{2\nu^2}} \quad (10)$$

with x defined as before. This parameterization has one free parameter, ν , which the authors set to 1.6 by fitting the SEY curve for five materials.

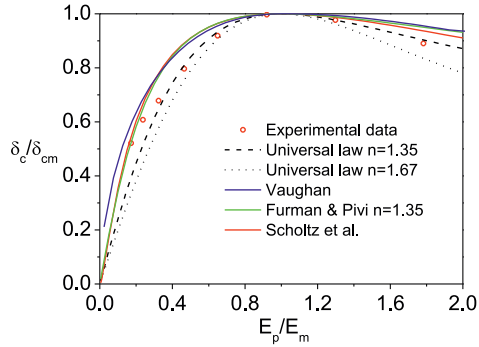


Fig. 3. Normalized corrected SEY, due only to true secondaries. The corrected experimental data are represented by dots, and the lines represent several parameterizations (see text).

It is worthy to note that the model leading to the semiempirical universal law considers the relation between the energy lost along the primary electron path in the medium and the secondary electron generation, without taking into account the electron flux reduction by backscattering. Vaughan [21] mentions the backscattered electrons as "a source of error that has not yet been considered". Scholtz et al. [13] correct their SEY data to compare them with the parameterizations, considering the ratio between true secondary current and primary current *entering* the medium, obtained subtracting the current of elastically reflected electrons from the primary current.

We will consider as the experimental magnitude directly comparable to the models the "corrected" secondary yield, δ_c , defined as the ratio of secondary electrons leaving the medium to the primary electrons entering the medium:

$$\delta_c = \frac{\delta}{1 - \eta_e}. \quad (11)$$

In eq. (11), the elastic yield η_e has been calculated from the measured spectra by a procedure explained in Section V. The influence of the factor $(1 - \eta_e)$ in eq. (11) decreases quickly as primary energy increases.

The data corrected that way along with the different parameterizations presented above are represented in Fig. 3. Both axes have been normalized to the curve maximum. The lower energy data ($E_p < 80$ eV) have not been included in the graph due to the difficulty to separate the true secondary and inelastic components in the spectra. The semiempirical universal law is represented for two values of n : 1.67 (Lin and Joy) and 1.35 (Seyler).

It can be seen that the formulas of Vaughan, Furman and Pivi, and Scholtz et al. give similar results, providing reasonable approximations to the Pt data in the represented energy range. Their estimations are, however, slightly higher than the data in the range 0.3-0.6 of normalized energies. The universal law provides worse results for $n = 1.67$ than for $n = 1.35$. In fact, the universal law with $n = 1.35$ is the parameterization that better fits the represented experimental data. However, it underestimates the SEY in the lower energy

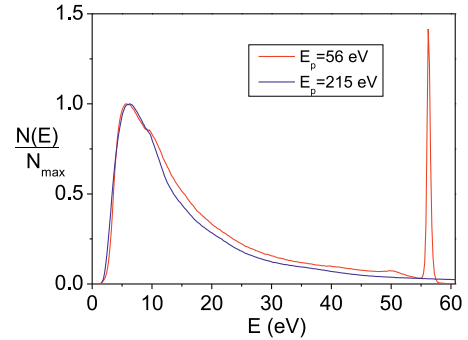


Fig. 4. Experimental Pt secondary spectra for 56 and 215 eV primary energies.

range ($E_p/E_m < 0.3$). This behavior for Pt ($Z=78$) is very similar for gold ($Z=79$), as shown in Fig. 3 of Scholtz et al.

Although the universal law with $n = 1.35$ provides a good description of the data in the represented energy range, several authors [20], [24] have pointed out that the high-energy ($E_p/E_m > 3$) SEY data are overestimated by this parameterization. Then, it can be concluded that the semiempirical universal law with $n = 1.35$ provides a good description of the SEY in the range $0.3 < E_p/E_m < 3$.

V. EXPERIMENTAL STUDY OF THE EMISSION SPECTRUM

In this section we present the results of the secondary ($E < 50$ eV) and elastic (events in the elastic peak) components of the emission spectrum, and the total backscattering yield (elastic and inelastic).

A. Secondary component

The secondary component of the emission spectrum is concentrated in the low-energy region, peaking at some eV. This makes the secondary spectrum especially sensitive to systematic errors associated to small offsets in the sample bias or in the analyzer. We have observed small deviations in the peaks and the rising edges when comparing spectra obtained for different primary energies. Two of these spectra, corresponding to primary energies of 56 and 215 eV and normalized to unit height, are shown in Fig. 4. A poorly defined shoulder can be observed at about 10 eV. The energy interval from the peak maximum to this shoulder takes approximately the same value (≈ 3.6 eV) for all spectra, irrespective of the primary energy. This suggests superposing the peaks to correct small experimental shifts. We have superposed all the spectra after normalizing their heights, forcing their peaks to coincide. A "mean" spectrum has been obtained that way whose peak is placed at an energy $E_{max} \approx 4.6$ eV relative to the sample vacuum level. The small deviations of E_{max} in the different spectra around this value show no correlation with the primary energy, and are thought to be due to experimental errors. Joy et al [25] give a value $E_{max} = 5$ eV for Pt. These authors give also the energy under which half of the secondary spectrum (up to 50 eV) area lies: 11 eV for Pt. In our spectra, this value ranges between 9 and 9.5 eV.

Although the main characteristics of the secondary spectrum below 10 eV do not depend significantly on E_p , the falling edge decreases more slowly for lower E_p values, as it can be seen in Fig. 4 by comparing the spectra for 56 and 215 eV. This seems to be due to the spreading of inelastically backscattered electrons over a narrower energy interval for lower E_p , resulting in a stronger contribution to the low energy spectrum, dominated by true secondaries.

A wide, low intensity peak can be seen in Fig. 4 near the elastic peak for the 56 eV spectrum. This wide peak is present in all spectra at energies about 5.5-5.7 eV under the elastic peak, and is thought to be due to plasmonic excitations.

Several theoretical or semiempirical parameterizations of the secondary spectrum shape have been published in the last four decades. We have compared our experimental spectra with three frequently used parameterizations, published by Chung and Everhart [26], Scholtz et al. [13], and Furman and Pivi [23].

The Chung-Everhart spectrum is

$$\frac{dN_s}{dE} = \frac{k}{E_p} \frac{E}{(E + \phi)^4}$$

where N_s is the number of secondary electrons of energy E , k is a normalization constant and ϕ is the work function of the medium (although comparison with experimental data yields values of ϕ significantly greater than typical work functions, see [25]). Using the normalized energy $u \equiv E/E_{max}$ and normalizing the spectrum to unit height, the previous expression reads

$$F(u) = u \left(\frac{4}{u+3} \right)^4 \quad (12)$$

where $F(u) \equiv (dN_s/du)/(dN_s/du)_{max}$. As it can be seen, after normalizing both axes, the Chung-Everhart spectrum does not contain any free parameter.

Scholtz et al. [13] found a reasonable fit between the secondary spectra of five materials and the following expression:

$$F(u) = e^{-\frac{ln^2 u}{2\tau^2}} \quad (13)$$

where we have used again normalized magnitudes in both axes. The parameter τ takes typical values between 0.7 and 1.1, as given by the authors.

Furman and Pivi [23] proposed the parameterization

$$F(u) = u^p \cdot e^{p(1-u)} \quad (14)$$

which has one free parameter using normalized magnitudes.

Fig. 5 shows the comparison between the experimental spectra and the parameterizations of Eqs. (12), (13) and (14). For the two last parameterizations, the free parameter has been selected by fitting the curves to the highest E_p spectrum (825 eV) from 0 to 50 eV, where the secondary component is the dominant one. The highest available E_p spectrum has been chosen trying to minimize the contribution of rediffused electrons to the spectrum, for reasons exposed before. It can be seen that the Chung-Everhart curve, although giving a reasonable approximation, overestimates the secondary spectrum, a result already noted by Joy et al. [25]. The Furman-Pivi curve provides a good approximation up to $4E_{max}$, but

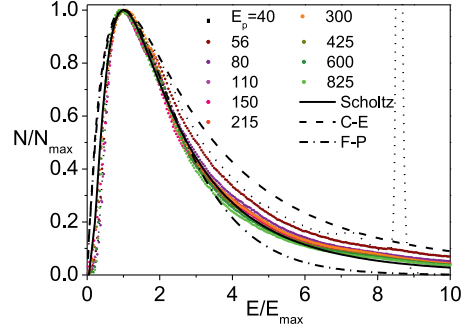


Fig. 5. Secondary emission spectra for primary energies between 40 and 825 eV. Three parameterizations are represented with the experimental data.

underestimates the spectrum for higher energies. The curve of Scholtz et al. seems to be the best parameterization in all the represented energy range (up to $10E_{max}$), including the rising edge, where the other curves behave clearly worse. The best-fit value of the parameter τ in the range 0-50 eV is 0.86, in the range of the values published by Scholtz et al.

B. Elastic component

The elastic fraction f_e of the emission spectrum, defined in Section I, can be obtained from the experimental spectra by comparing the events contained in the elastic peak and the total number of events. However, to be representative of the total emission, the spectra have to be measured by an analyzer with an acceptance solid angle close to the 2π steradians of the half-sphere over the sample. Our analyzer, placed at 45° to the sample normal, accepts a solid angle close to 0.16 sr, and therefore the measured spectra are representative of a set of directions around 45° . We will denote as f_{em} the elastic fractions obtained from the spectra measured at 45° , and f_e the elastic fractions of the whole emission. The same notation will be used for the inelastic and secondary components. The relation between f_k and f_{km} , with $k = \{\text{elastic, inelastic and secondaries}\}$, can be established through the probability $p_k(\Delta\Omega)$ that an electron leaving the surface after a process k has an emission direction in the solid angle $\Delta\Omega$ of the analyzer. It is straightforward to show that:

$$f_{km} = \frac{f_k p_k(\Delta\Omega)}{\sum_{k=e,i,s} f_k p_k(\Delta\Omega)}. \quad (15)$$

If the $p_k(\Delta\Omega)$ are known, eq. (15) can be unfolded to obtain f_k from f_{km} . These probabilities have been calculated by Monte Carlo simulation using suitable angular emission distributions. For the secondary and inelastic angular distributions we have employed a $\cos\theta$ law (Lambert's law). For the angular distribution of elastic electrons we have interpolated our measured primary energies in experimental angular distributions [27]–[29], corresponding to primary energies between 100 and 1000 keV. The two lower-energy spectra (40 and 56 eV) have not been corrected due to the lack of reliable data.

The elastic fraction obtained directly from the spectra, that is, uncorrected (f_{em}), and the corrected elastic fraction

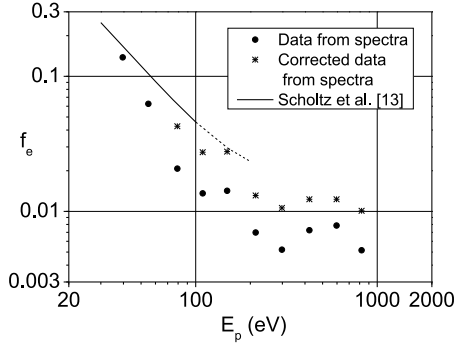


Fig. 6. Elastic fraction for Pt. Dots: raw experimental data. Crosses: corrected data (see text). Line: parameterization (16) extended up to 200 eV.

(f_e) are shown in Fig. 6. The continuous line in this graph represents the parameterization proposed by Scholtz et al. [13] for primary energies E_p lower than 100 eV:

$$\ln f_e(\%) = 1.59 + 3.75 \ln E_p - 1.37(\ln E_p)^2 + 0.12(\ln E_p)^3. \quad (16)$$

This parameterization has been represented up to 200 eV (discontinuous line), 100 eV further than the range proposed by Scholtz et al., to show the trend of f_e . Although the trends shown by the corrected data and the parameterization are similar, the data lie clearly under the curve. This could be due to deviations of the inelastic angular distribution from Lambert's law in the unfolding of eq. (15). Unfortunately, a great lack of experimental information exists about the inelastic angular distributions.

With the measured values of σ and f_e we can obtain the elastic contribution to the total yield using eq. (5). We now pass to compare our η_e experimental data with two empirical formulas.

De Lara et al. [30] proposed the following dependence of η_e with E_p and the atomic number Z :

$$\eta_e(E_p) = \frac{p_0 - 0.07}{1 + \frac{E_p}{E_1}} + \frac{0.07}{1 + \frac{E_p}{E_2}} \quad (17)$$

where p_0 is the probability of elastic reflection for very low primary energies, which the authors take as 1. The other parameters are defined as

$$E_1(\text{eV}) = \frac{50}{\sqrt{Z}} \quad E_2(\text{eV}) = 0.25Z^2.$$

Furman and Pivi [23] propose a parameterization with five free parameters. However, for the two materials studied in their paper (copper and stainless steel), one parameter is zero and another one is around one. Therefore, for the sake of simplicity, we can use a simplified parameterization with three free parameters:

$$\eta_e(E_p) = p_\infty + (p_0 - p_\infty)e^{-\frac{E_p}{W}}. \quad (18)$$

In table III we list the parameters given by Furman and Pivi [23] for copper and stainless steel, along with the best fit parameters of this model to our data. The data and the two parameterizations mentioned here are represented against the primary energy in Fig. 7.

TABLE III
BEST-FIT PARAMETERS OF EQ. (18) FOR THREE MATERIALS.

	p_0	p_∞	W (eV)
Cu[23]	0.496	0.02	60.86
Steel[23]	0.5	0.07	100
Pt (this work)	0.468	0.0136	21.4

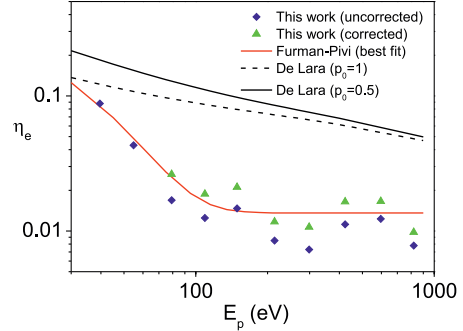


Fig. 7. Elastic component of the total SEY. Comparison between experimental data and parameterizations (see text).

C. Backscattering coefficient

As mentioned in Section I, the elastic and inelastic backscattering yields are usually joined in the backscattering coefficient (eq.(5)). We have measured η following the procedure described in Section III. The results are shown in Fig. 8 along with the measurements of El Gomati et al. [31] for Pt. The graph includes also the parameterization of Dapor [32], valid up to 6.7 keV and normal incidence:

$$\eta = 1 - \frac{1 + 3\varepsilon\sqrt{Z-1}}{(1 + \varepsilon\sqrt{Z-1})^3} \quad (19)$$

where Z is the atomic number and

$$\varepsilon = 0.0811 + 0.0037E_p(\text{keV}).$$

Although there are some discrepancies between our experimental results and those of El Gomati, the trend is similar: a monotonic increase with energy that slows down when approaching the keV region. This is consistent with the measured data of Yadav and Shanker [33] for Pt (8-28 keV) at normal incidence, suggesting an asymptotic value close to 0.5 at high primary energies. The experimental results suggest that the Dapor formula is not adequate for primary energies under 500 eV, at least for high atomic numbers. The constant additive term in ε prevents η to decrease with decreasing E_p as fast as the data indicate.

VI. CONCLUSIONS

The SEY and SES of clean Pt have been measured for normal incidence and primary energies lower than 1 keV. The measured magnitudes have been compared with theoretical or semiempirical formulas. Although the SEY formulas of Vaughan, Furman and Pivi, and Scholtz et al. provide reasonable approximations in the analyzed energy range, the

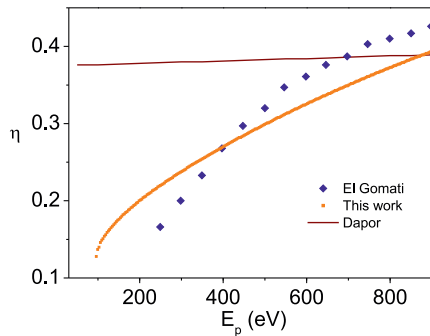


Fig. 8. Backscattering coefficient for Pt: experimental results and Dapor formula.

semiempirical universal law with $n = 1.35$ provides a better description of the corrected SEY of Pt. The peak of the secondary emission for Pt is close to 4.6 eV referred to the vacuum level at the sample. The spectral shape is better described by the empirical formula of Scholtz et al. than by the theoretical formula of Chung and Everhart or by the empirical formula of Furman and Pivi. Our measurements of the elastic fraction for Pt are lower than, although not far from, the results of the Scholtz et al. empirical formula in its validity range (< 100 eV). The elastic yield measurements are better described by the empirical formula of Furman and Pivi than by the empirical formula of De Lara et al. The backscattering coefficient data we have obtained for Pt show a trend to increase and saturate with energy similar to those of El Gomati et al. The semiempirical expression of Dapor predicts the high energy value of the backscattering coefficient but it does not describe the energy dependence in the low-energy region.

ACKNOWLEDGMENT

This work was supported by the MINECO under the Research Project TEC2013-47037-C5-4-R, and by the MICIIN under the Research Project AYA2012-39832-C02-01/02 (Space Programme). Our acknowledgement to the EH-PSML of Val Space Consortium.

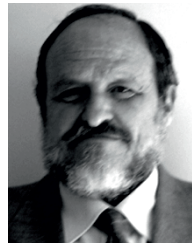
REFERENCES

- [1] N. Rozario, H. F. Lenzing, K. F. Reardon, M. S. Zarro, and C. G. Baran, "Investigation of telstar 4 spacecraft Ku-band and C-band antenna components for multipactor breakdown," *IEEE Trans. Microwave Theory Tech.*, vol. 42, no. 3, pp. 558–564, Apr. 1994.
- [2] C. Vicente, M. Mattes, D. Wolk, B. Mottet, H. L. Hartnagel, J. R. Mosig, and D. Raboso, "Multipactor breakdown prediction in rectangular waveguide based components," *Proceedings of the 2005 IEEE MTT-S International Microwave Symposium*, pp. 1055–1058, 2005.
- [3] S. Yamaguchi, Y. Saito, S. Anami, and S. Michizono, "Trajectory simulation of multipactoring electrons in an S-band pillbox RF window," *IEEE Trans. Nucl. Sci.*, vol. 39, no. 2, pp. 278–282, Apr. 1992.
- [4] L. K. Ang, Y. Y. Lau, R. A. Kishkek, and R. M. Gilgenbach, "Power deposited on a dielectric by multipactor," *IEEE Trans. Plasma Sci.*, vol. 26, no. 3, pp. 290–295, Jun. 1998.
- [5] M. Ito, H. Kume, and K. Oba, "Computer analysis of the timing properties in micro channel plate photomultiplier tubes," *IEEE Trans. Nucl. Sci.*, vol. NS-31, no. 1, pp. 408–412, Feb. 1984.
- [6] H. Seiler, "Secondary electron emission in the scanning electron microscope," *J. App. Phys.*, vol. 54, 1983.

- [7] L. Reimer, *Scanning electron microscopy physics of image formation and microanalysis*. Springer, 1995.
- [8] H. B. Garrett, "The charging of spacecraft surfaces", *Rev. Geophys. Space Phys.*, vol. 19, no. 4, pp. 577–616, 1981.
- [9] N. Nickles, R. E. Davies, and J. R. Dennison, "Applications of secondary electron energy- and angular-distributions to spacecraft charging", *6th Spacecraft Charging Technology Conference*, pp. 275–280, 2000.
- [10] S. Jurac, R. A. Baragiola, R. E. Johnson, and E. C. Sittler Jr., "Charging of ice grains by low-energy plasmas: Application to Saturn's E ring," *J. Geophys. Res.: Space Phys.*, vol. 100, no. A8, pp. 14821–14831, Aug. 1995.
- [11] R. G. Lye, and A. J. Dekker, "Theory of secondary emission", *Phys. Rev.*, vol. 107, pp. 977–981, 1957.
- [12] G. F. Dionne, "Origin of secondary-electron-emission yield-curve parameters", *J. Appl. Phys.*, vol. 46, no. 8, pp. 3347–3351, 1975.
- [13] J. J. Scholtz, D. Dijkkamp, and R. W. A. Schmitz, "Secondary emission properties", *Philips J. Res.*, vol. 50, pp. 375–389, 1996.
- [14] Y. Lin, and D. C. Joy, "A new examination of secondary electron yield data", *Surf. Interface Anal.*, vol. 37, pp. 895–900, 2005.
- [15] H. Bruining, *Physics and Applications of Secondary Electron Emission*. McGraw-Hill, 1954.
- [16] A. Endo, and S. Ino, "Energy and angular distribution of secondary electrons emitted from $Si(111) - 7 \times 7, \sqrt{3} \times \sqrt{3} - Ag$ and $5 \times 2 - Au$ surfaces", *Surf. Science*, vol. 346, pp. 40–48, 1996.
- [17] C. G. H. Walker, M. M. El-Gomati, A. M. D. Assa'd, and M. Zdražil, "The Secondary Electron Emission Yield for 24 Solid Elements Excited by Primary Electrons in the Range 2505000 eV: A Theory/Experiment Comparison", *Scanning*, vol. 30, pp. 365–380, 2008.
- [18] J. Krim, I. Heyvaert, C. Van Haesendonck, and Y. Bruynseraede, "Scanning tunneling microscopy observation of self-affine fractal roughness in ion-bombarded film surfaces", *Phys. Rev. Lett.*, vol. 70, no. 1, pp. 57–60, 1993.
- [19] S. Clerc, J. R. Dennison, R. Hoffmann and J. Abbott, "On the Computation of Secondary Electron Emission Models", *IEEE Trans. Plasma Sci.*, vol. 34, no. 5, pp. 2219–2225, 2006.
- [20] N. Bundaleski, B. J. Shan, A. G. Silva, A. M. C. Moutinho, and O. M. N. D. Teodoro, "Novel Approach to the Semi-Empirical Universal Theory for Secondary Electron Yield", *Scanning*, vol. 33, pp. 1–4, 2011.
- [21] R. Vaughan, "A New Formula for Secondary Emission Yield", *IEEE Trans. Elec. Devices*, vol. 36, pp. 1963–1967, 1989.
- [22] R. Vaughan, "Secondary Emission Formulas", *IEEE Trans. Elec. Devices*, vol. 40, p. 830, 1993.
- [23] M. A. Furman, and M. T. F. Pivi, "Probabilistic model for the simulation of secondary electron emission", *Phys. Rev. ST Accel. Beams*, vol. 5, p. 124404, 2002.
- [24] S. A. Schwarz, "Application of a semi-empirical sputtering model to secondary electron emission", *J. Appl. Phys.*, vol. 68, pp. 2382–2391, 1990.
- [25] D. C. Joy, M. S. Prasad and H. M. Meyer, "Experimental secondary electron spectra under SEM conditions", *Journal of Microscopy*, vol. 215, pp. 77–85, 2004.
- [26] M. S. Chung, and T. E. Everhart, "Simple calculation of energy-distribution of low-energy secondary electrons emitted from metals under electron bombardment", *J. Appl. Phys.*, vol. 45, no. 2, pp. 707–709, 1974.
- [27] A. Jablonski, and P. Jiricek, "Elastic Electron Backscattering from Surfaces at Low Energies", *Surface and Interface Analysis*, vol. 24, pp. 781–785, 1996.
- [28] A. Jablonski, "Elastic electron backscattering from gold", *Phys. Rev. B*, vol. 43, no. 10, pp. 7546–7554, 1991.
- [29] A. Jablonski, "Analytical theory of elastic electron backscattering from elements, alloys and compounds: Comparison with experimental data", *Journal of Electron Spectroscopy and Related Phenomena*, vol. 206, pp. 24–45, 2016.
- [30] J. de Lara, F. Pérez, M. Alfonso, L. Galán, I. Montero, E. Román and D. Raboso Garcia Baquero, "Multipactor prediction for on-board spacecraft RF equipment with the MEST software tool", *IEEE Trans. Plasma Sci.*, vol. 34, no. 2, pp. 476–484, 2006.
- [31] M. M. El Gomati, C. G. H. Walker, A. M. D. Assa'd and M. Zdražil, "Theory experiment comparison of the electron backscattering factor from solids at low electron energy (250–5000 eV)", *Scanning*, vol. 30, pp. 2–15, 2008.
- [32] M. Dapor "Theory of the interaction between an electron beam and a thin solid film", *Surf. Sci.*, vol. 269/270, pp. 753–762, 1992.
- [33] R. K. Yadav, and R. Shanker, "Backscattering of 828 keV electrons from a thick Al, Ti, Ag and Pt targets", *J. Electr. Spectrosc. Relat. Phenom.*, vol. 151, pp. 71–77, 2006.



Enrique Bronchalo was born in Guadalajara (Spain) in 1963. He received the Physics degree from the Universidad Complutense de Madrid in 1986, and the Ph.D. on Physics from the Universidad de Alcalá in 1996. In 2001 he joined the Departamento de Ingeniería de Comunicaciones at the Universidad Miguel Hernández de Elche, (Elche, Spain), where he occupies an Associate Professor position. His current research is focused on passive microwave devices and multipactor processes in waveguides.



Luis Galán received the Ph.D. degree in materials science and engineering from Stanford University, Stanford, CA, in 1980. He is Associate Professor in the Universidad Autónoma de Madrid, Madrid, Spain. He has published over 80 research papers. His present interest is in secondary emission properties of materials with application in space hardware, in relation with multipactor breakdown, including micro- and nano-structured surfaces.



Ángela Coves was born in Elche (Alicante), Spain, in 1976. She received the Licenciado degree in Physics and the Ph.D degree in Physics from the Universidad de Valencia, Valencia, Spain, in 1999 and 2004, respectively. She became a Lecturer at the Universidad Miguel Hernández de Elche in 2001. Her current research interests are focused on the analysis and design of microwave passive components, periodic structures and RF breakdown high-power effects.



Vicente E. Boria (S91-A99-SM02) was born in Valencia, Spain, in 1970. He received his Ingeniero de Telecomunicación degree and the Ph.D degree from the Universidad Politécnica de Valencia, Valencia, Spain, in 1993 and 1997, respectively. He became a Full Professor at the Universidad Politécnica de Valencia in 2003. His research interests include the analysis and automated design of passive components, left-handed and periodic structures, and power effects in passive waveguide systems.



Rafael Mata received the Degree in Physics and the Ph.D. degree from the University of Valencia, Valencia, Spain, in 2006 and 2011, respectively. He obtained a researcher/technician position in 2012 to work in the Val Space Consortium. His current research activities are related with the secondary electron emission properties, outgassing and venting processes in RF high power space materials.



Laura Mercadé received the Degree in Physics from the University of Valencia, Valencia, Spain, in 2015 and in 2016 she will finalize a Master in Advanced Physics in the same University. She obtained a technical student position at CERN in 2016. Her current research activities are related with the RF breakdown phenomena in DC and RF structures and the secondary electron emission properties.



Benito Gimeno (M01) received the Licenciado degree in physics and the Ph.D. degree from the University of Valencia, Valencia, Spain, in 1987 and 1992, respectively. He became a Full Professor at the University of Valencia in 2010. His current research interests include the electromagnetic analysis and design of microwave passive components, and RF breakdown high-power effects.



Isabel Montero is currently Research Professor of the Spanish National Research Council (CSIC), Spain. She is head of the Group Surface Nanostructuring for Space and Terrestrial Communications of the Materials Science Institute of Madrid (ICMM-CSIC). She is director of Spanish laboratory on secondary electron emission (SEY) of CSIC. She is expert in surface spectroscopic techniques, and in low- secondary electron emission surfaces and coatings to avoid multipaction effect.



Esteban Sanchís-Kilders (M'00-SM'14) was born in Valencia, Spain. He received the M.Sc. degree in physics, with specialization in electronics, and the Ph.D. degree from the University of Valencia, Spain, in 1990 and 1997, respectively. He is currently Associate Professor at the University of Valencia. His main research interests are space systems and new electronic devices applied to space applications.